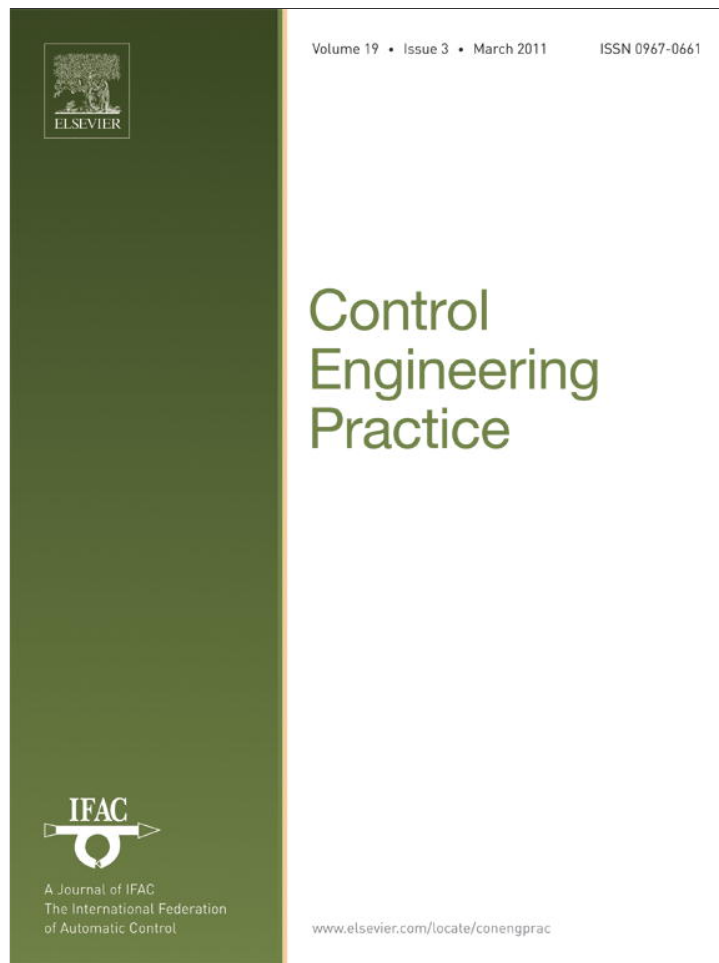


Provided for non-commercial research and education use.
Not for reproduction, distribution or commercial use.



This article appeared in a journal published by Elsevier. The attached copy is furnished to the author for internal non-commercial research and education use, including for instruction at the authors institution and sharing with colleagues.

Other uses, including reproduction and distribution, or selling or licensing copies, or posting to personal, institutional or third party websites are prohibited.

In most cases authors are permitted to post their version of the article (e.g. in Word or Tex form) to their personal website or institutional repository. Authors requiring further information regarding Elsevier's archiving and manuscript policies are encouraged to visit:

<http://www.elsevier.com/copyright>



ELSEVIER

Contents lists available at ScienceDirect

Control Engineering Practice

journal homepage: www.elsevier.com/locate/conengprac

Iterative learning control of molten steel level in a continuous casting process

Byungyong You^a, Minsung Kim^a, Dukman Lee^b, Jookang Lee^a, J.S. Lee^{a,*}^a Department of Electrical and Electronic Engineering, Pohang University of Science and Technology, Pohang 790-784, Republic of Korea^b Technical Research Laboratories, Pohang Iron and Steel Co., Ltd., 790-785, Pohang, Republic of Korea

ARTICLE INFO

Article history:

Received 18 June 2009

Accepted 18 November 2010

Available online 6 January 2011

Keywords:

Iterative learning control

Continuous casting

Molten steel level

Switching control

Forgetting factor

ABSTRACT

In this paper, an iterative learning control (ILC) method is introduced to control molten steel level in a continuous casting process, in the presence of disturbance, noise and initial errors. The general ILC method was originally developed for processes that perform tasks repetitively but it can also be applied to periodic time-domain signals. To propose a more realistic algorithm, an ILC algorithm that consists of a P-type learning rule with a forgetting factor and a switching mechanism is introduced. Then it is proved that the input signal error, the state error and the output error are ultimately bounded in the presence of model uncertainties, periodic bulging disturbances, measurement noises and initial state errors. Computer simulation and experimental results establish the validity of the proposed control method.

© 2010 Elsevier Ltd. All rights reserved.

1. Introduction

In continuous casting of steel, controlling the molten steel level is very important because a consistent level increases the surface quality of the final products. However, the level of molten steel in continuous casters is affected by disturbances, time delays and nonlinearities. In a continuous caster, one of the most severe disturbances is bulging, which disturbs the level periodically. Normally, bulging is similar in shape to a superposition of sinusoidal waves and causes molten steel level to oscillate periodically. This paper focuses mainly on eliminating bulging disturbance.

Many strategies have been proposed to control the level of molten steel during continuous casting (Barron, Aguilar, Gonzalez, & Melendez, 1998; Dussud, Galichet, & Foulloy, 1998; Keyser, 1991; Lee, Kueon, & Lee, 2003; Watanabe, Omura, Konishi, Watanabe, & Furukawa, 1999), but none of these attempts to eliminate bulging disturbance directly. Furtmueller and Gruenbacher (2006) modeled the bulging effect and applied it to his control strategy, but this method requires measurement of the current signal of the roller motor under the mold, but this is difficult to obtain in the field and does not properly reflect mold level disturbance due to bulging. Therefore, an iterative learning controller is proposed that can be applied easily to controlling molten steel level.

In a system that is subject to periodic disturbance, the repetitive control method (Doh, Ryoo, & Chung, 2006; Moon, Lee, & Chung,

1998) is often useful. However the repetitive controller needs precise plant information for stability, and large time delay significantly degrades its performance. In contrast, ILC method does not need any plant information, and is easy to implement even in systems that experience large time delay. The proposed ILC technique is responsible for eliminating bulging disturbance while the PID controller mainly stabilizes molten steel level.

This paper is organized as follows. Section 2 derives a mathematical model for molten steel level system; Section 3 describes the proposed controller and the resulting control system; Section 4 shows computer simulation results and Section 5 shows experimental results on 1/4 scale hardware (H/W) simulator; the conclusion is given in Section 6; the stability analysis on the control system is given in the Appendix.

In this paper, the following notations and definitions will be used. \mathbb{R}^n is the n -dimensional Euclidean space with norm $\|z\| = (z^T z)^{1/2}$ for $z \in \mathbb{R}^n$. $C \in \mathbb{R}^{p \times m}$ is a $(p \times m)$ -dimensional matrix with real elements and $\|C\| = \sqrt{\lambda_{\max}(C^T C)}$ represents the induced matrix norm where $\lambda_{\max}(\cdot)$ denotes the maximum eigenvalue. Let \mathbb{N} be the set of positive integers $1, 2, \dots, n$. Finally, the α -norm is defined for a positive real function $z: \mathbb{N} \rightarrow \mathbb{R}$ as

$$\|z(\cdot)\|_{\alpha} = \sup_{k \in \mathbb{N}} z(k) \left(\frac{1}{\alpha}\right)^k \quad \text{for } \alpha \geq 1.$$

2. Molten steel level model

In the continuous casting process (Fig. 1), the molten steel in the tundish (Fig. 2) is poured into the mold through a nozzle. The control process is activated to maintain the molten steel level at a preset value. The molten steel is cooled first in the mold, and then

* Corresponding author.

E-mail addresses: ybyvic@postech.ac.kr (B. You), redtoss@postech.ac.kr (M. Kim), drdmlee@posco.co.kr (D. Lee), jkleee@postech.ac.kr (J. Lee), jsoo@postech.ac.kr (J.S. Lee).

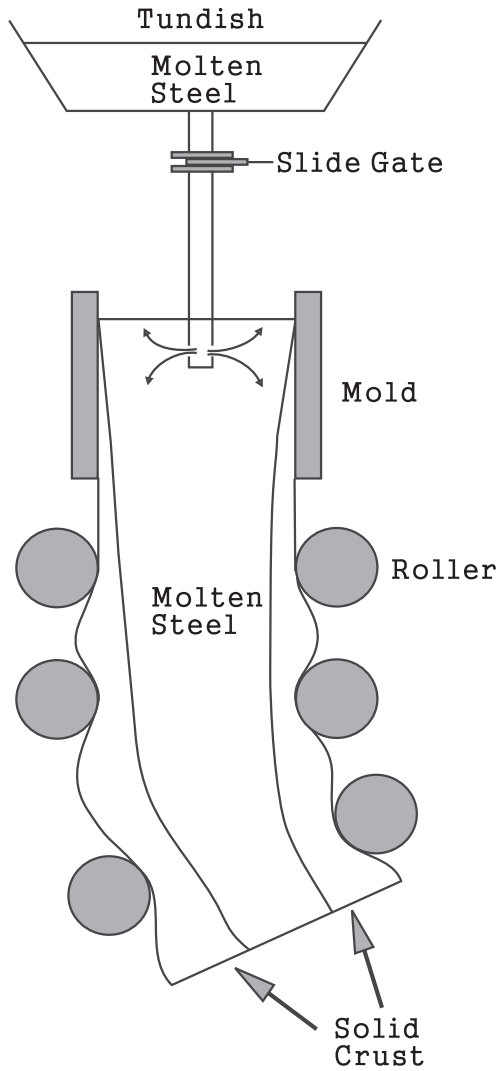


Fig. 1. Continuous casting process.

further by cooling units in the rolls under the mold. Finally the molten steel is shaped into slabs after passing through many rollers.

The continuity equation of the molten steel in the mold is

$$\frac{dV}{dt} = Q_{in} - Q_{out}, \quad (1)$$

where Q_{in} (m^3/s) is the incoming molten steel flow into the mold, Q_{out} (m^3/s) is the outgoing flow from the mold, and V (m^3) is the volume of molten steel stored in the mold. V is represented as $A \times y$, where A (m^2) is the cross sectional area of the mold and y (m) is the molten steel level in the mold. $A = W \cdot D$, where W (m) is the width of the mold and D (m) is its thickness. Then, Eq. (1) becomes

$$\frac{dy}{dt} = \frac{1}{A} (Q_{in} - Q_{out}), \quad (2)$$

where Q_{in} and Q_{out} are represented as

$$Q_{in} = \sqrt{2gh}SG(u),$$

$$Q_{out} = A \cdot v_0. \quad (3)$$

Here, g (m/s^2) is the gravity acceleration; $\sqrt{2gh}$ is the outgoing velocity of molten steel from the tundish; h (m) is the height of molten steel in the tundish; $SG(u)$ (m^2) is the cross-sectional area through which molten steel flows into the mold and v_0 (m/s) is the

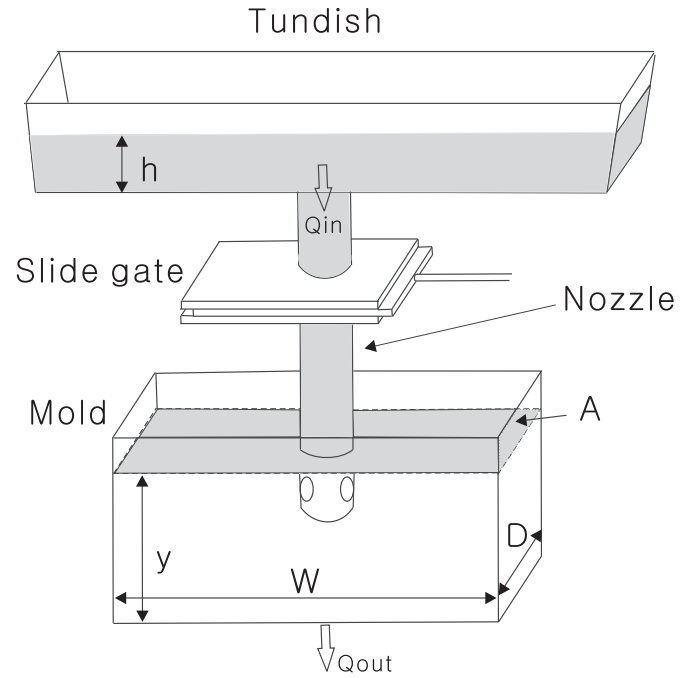


Fig. 2. Tundish and mold.

casting speed. $SG(u)$ can then be calculated as

$$SG(u) = 0, \quad u \leq z,$$

$$SG(u) = 4 \int_{(u+b)/2}^{u+r} \sqrt{r^2 - (x-u)^2} dx, \quad u > z$$

$$= \pi r^2 - 2r^2 \arcsin\left(\frac{b-u}{2r}\right) - \left(\frac{b-u}{2}\right) \sqrt{4r^2 - (b-u)^2}, \quad (4)$$

where u (m) is the input reference of the slide gate; z (m) is the dead zone; r (m) is the radius of the slide gate; b (m) is the maximum moving distance of the slide gate.

The molten steel level model, (2)–(4) can be described as

$$x_i(k+1) = x_i(k) + B(x_i(k), u_i(k), k) + \beta_i(k) + d_i(k),$$

$$y_i(k) = x_i(k) + n_i(k), \quad (5)$$

where i indicates the number of iterations, k is the discrete time index starting from $k=1$ to $k=n$. For all $k \in \mathbb{N}$, $x_i(k) \in \mathbb{R}^p$, $u_i(k) \in \mathbb{R}^r$, $y_i(k) \in \mathbb{R}^m$, $\beta_i(k) \in \mathbb{R}^p$, $d_i(k) \in \mathbb{R}^p$, $n_i(k) \in \mathbb{R}^m$ are, respectively, the state, the input, the output, the model uncertainty, the periodic bulging disturbance and the output measurement noise at the i th iteration. $B(x_i(k), u_i(k), k)$ is equal to $(\Delta T/A)(\sqrt{2gh}SG(F_{fb}(u_i(k))) - Q_{out})$ where ΔT is the sampling time and $F_{fb}(\cdot)$ is a function of the control input. The molten steel level equation (5) satisfies the following properties and bounds.

Property 1. A target trajectory for the iterative learning algorithm is given as a bounded output sequence $y_d(k)$, $k \in \mathbb{N}$, that can be represented as

$$x_d(k+1) = x_d(k) + B(x_d(k), u_d(k), k),$$

$$y_d(k) = x_d(k). \quad (6)$$

Property 2. The function $B(x_i(k), u_i(k), k)$ is globally Lipschitz with respect to $x_i(k), u_i(k)$:

$$\|B(x_1, u_1, k) - B(x_2, u_2, k)\| \leq c_B(\|x_1 - x_2\| + \|u_1 - u_2\|) \quad (7)$$

for all $k \in \mathbb{N}$ and for some positive constant c_B .

Property 3. The function $B(x_i(k), u_i(k), k)$ is bounded as $\|B(x_i(k), u_i(k), k)\| \leq b_B$, where b_B is a positive constant.

In developing the controller, three assumptions on the system are imposed as follows:

Assumption 1.

$$\max_{1 \leq k \leq n} \|u_d(k)\| \leq b_{u_d}$$

Assumption 2. The disturbances and noises are bounded as

$$\max_{1 \leq i < \infty} \max_{1 \leq k \leq n} \|\beta_i(k)\| \leq b_\beta,$$

$$\max_{1 \leq i < \infty} \max_{1 \leq k \leq n} \|d_i(k)\| \leq b_d,$$

$$\max_{1 \leq i < \infty} \max_{1 \leq k \leq n} \|n_i(k)\| \leq b_n,$$

for some positive constants b_β, b_d, b_n .

Assumption 3. For every iteration, the trajectory starts within a neighborhood of $x_d(0)$ such that $\|x_d(0) - x_i(0)\| \leq b_{x_0}$ for all $i \geq 1$ and for some $b_{x_0} > 0$.

These assumptions normally hold for most repetitive nonlinear dynamic systems (Hauser, 1987; Heinzinger, Fenwick, Paden, & Miyazaki, 1992; Jang, Choi, & Ahn, 1995; Kang, Lee, & Han, 2005; Kuc, Lee, & Nam, 1992; Wang, 1998). Assumption 3 is normally satisfied because the PID controller mainly stabilizes the output signal, and because the initial state of the bulging disturbance is usually close to the desired output signal.

3. Controller design

An iterative learning rule is proposed for control of the molten steel level during the continuous casting process:

$$u_{i+1}(k) = s_{i1}(k)[(1-p)u_i(k) + L(k)e_i(k+1)] + s_{i2}(k)[u_{i+1}(k-1)], \quad (8)$$

for the i th iteration, where $e_i(k) = y_d(k) - y_i(k)$ are the output tracking errors, $s_{i1}(k) = 0.5[\text{sgn}(T_v - e_{i+1}(k)) + 1]$, $s_{i2}(k) = -0.5[\text{sgn}(T_v - e_{i+1}(k)) - 1]$, T_v is a threshold value used for switching mechanism, $L(k)$ is the learning gain that satisfy $L(k) \leq b_L$ for all $k \in \mathbb{N}$ and for some b_L , and p is a forgetting factor (Chien & Liu, 1994; Heinzinger et al., 1992) that satisfies $0 \leq p < 1$. Obviously, $p=0$ corresponds to integral action, and $0 < p < 1$ corresponds to low pass filtering in the iteration domain. $u_i(k) + L(k)e_i(k+1)$ is the typical predictive learning term. When the level error is smaller than the threshold value in the switching controller, a P-type learning rule is used with a forgetting factor. If the level error exceeds the threshold value, then the input maintains the previous one.

In the proposed control system (Fig. 3), the PID controller is responsible for overall control stability. Because bulging disturbance is periodic, one period is treated as one iteration and apply

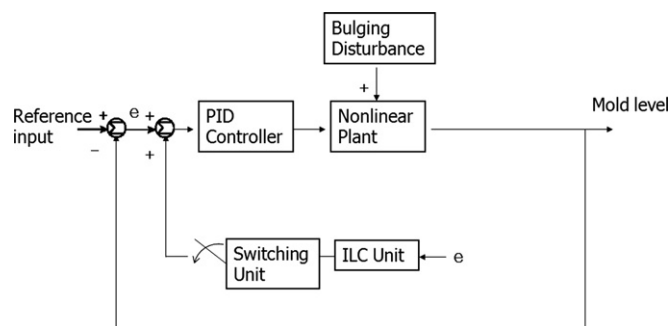


Fig. 3. Proposed control system.

ILC during each period. Bulging disturbance frequencies can be calculated from the roll pitch and casting speed information, or can be determined by performing a fast Fourier transform (FFT).

In a molten steel level system, periodic bulging is usually generated by periodic shrinkage and expansion of molten steel when it passes through the casting rollers below the mold. When the molten steel passes through the rollers, the unsolidified part expands when between them and shrinks when in contact with them. This bulging disturbance is directly translated into variation in the molten steel level in the mold, which cannot be easily regulated using conventional control methods.

Periodic bulging is generally composed of two sine waves with almost identical amplitudes, but each peak of the bulging disturbance may not be exactly the same in all iterations (Fig. 4). Particularly around the small amplitude area, the small errors can cause sign changes in successive iterations, thereby causing significant errors in the level of the molten steel. To overcome this problem, a forgetting factor and a switching mechanism are introduced in the proposed algorithm. The forgetting factor reduces the effect of the current input signal, particularly when this signal is computed from an error-prone disturbance; the switching controller turns off the ILC unit when the output level exceeds a threshold value. These two control strategies are useful in general because the bulging disturbance varies over time (see Fig. 5).

Another concern is that the molten steel level system experiences significant time delay. If this time delay ignored, the

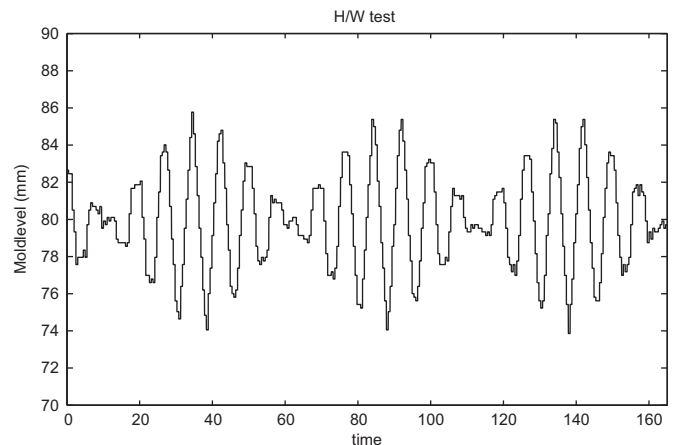


Fig. 4. Bulging disturbance generated from the H/W simulator.

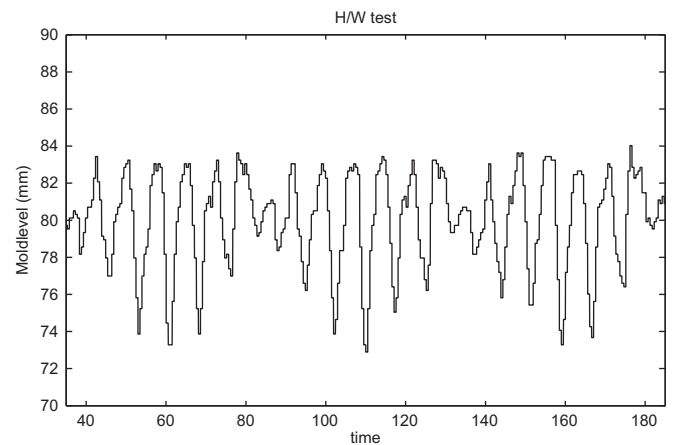


Fig. 5. Mold level output.

performance of various control methods can deteriorate or even diverge. The system time delay can be measured directly; it measured so in 1/4 scale H/W simulator (Fig. 6). First, an input sinusoidal signal is applied off-line to the slide gate with the same frequency as that of the bulging and then measured the time difference between the input slide gate signal and the output mold level signal. Then the resulting time delay can be measured (Fig. 6),

and was about 2 s in the case of 1/4 scale H/W simulator. The ILC algorithm can easily compensate for time delay by generating a control input and applying it to the system in advance of the disturbance by an interval equivalent to the measured time delay. This process causes the ILC algorithm to be in phase with the mold level system, thereby compensating for the bulging disturbance.

Still another concern is the difficulty in finding the starting point when applying the ILC algorithm. This starting point can be found by examining the mold level signal of the PID control system. Because the level signal is periodic (Fig. 6), the starting point can be selected manually or determined automatically by using the computer algorithm. Once the starting point is located, the subsequent starting points of the periodic signal can be determined automatically by using information about the bulging disturbance frequency. In the presence of model uncertainties, disturbances, noises and initial errors, we can prove that the state signal error, the output signal error and the input signal error of the control system are ultimately bounded, the proof of which is given in the Appendix.

4. Simulation results

To demonstrate the feasibility of the developed controller, a simulation is performed. The reference mold level was set to 80 mm, reflecting the desired level of the hardware simulator. The

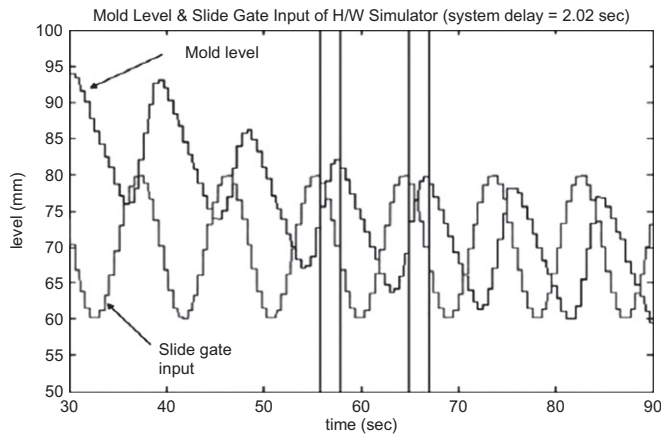


Fig. 6. System delay measurement.

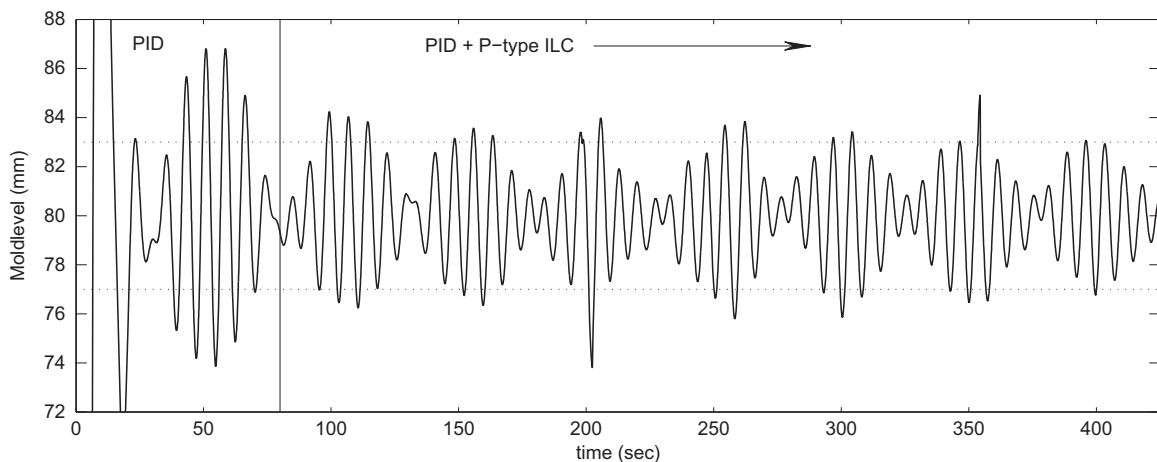


Fig. 7. Simulation result of the PID and P-type ILC control system.

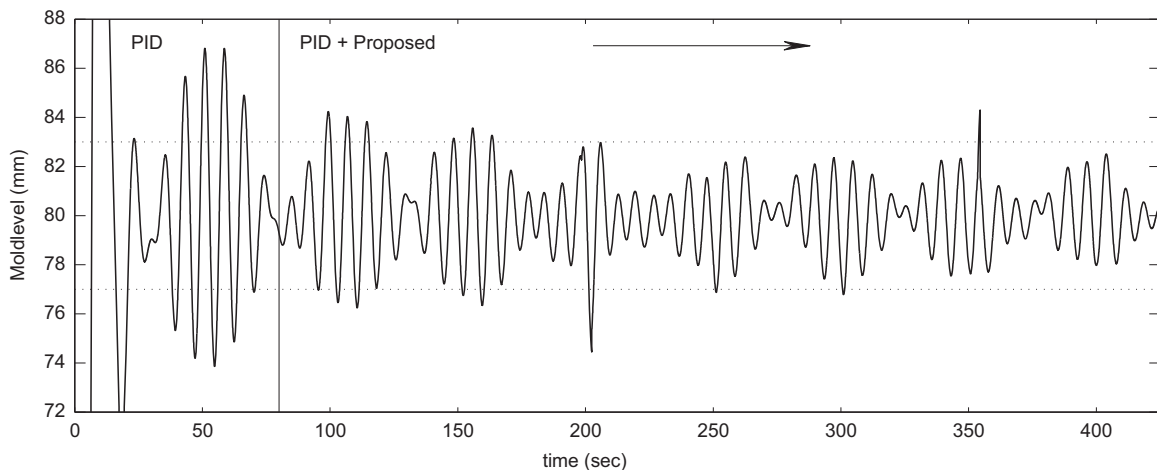


Fig. 8. Simulation result of the PID and proposed control system.

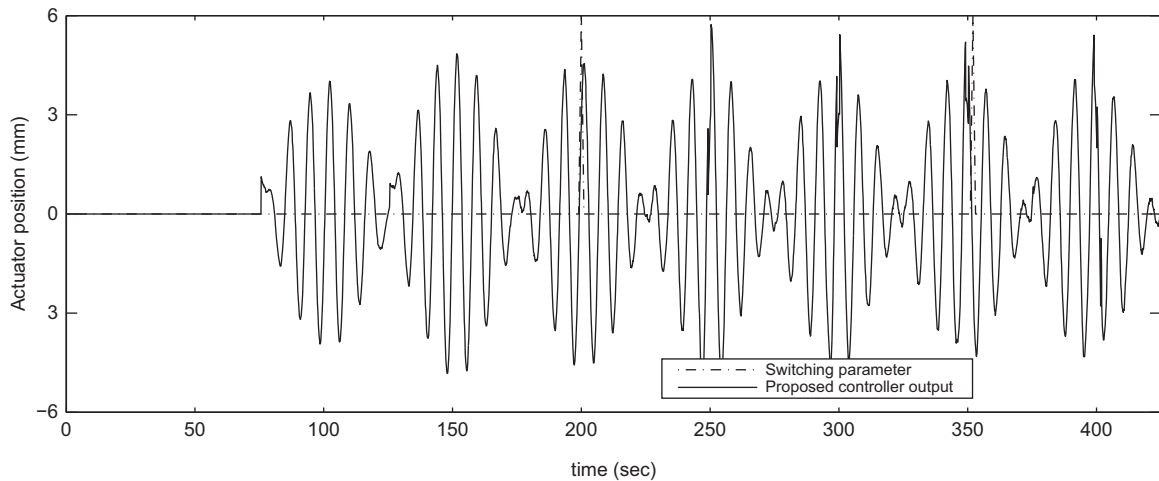


Fig. 9. The switching parameter $s_2(k)$ and the proposed controller output.

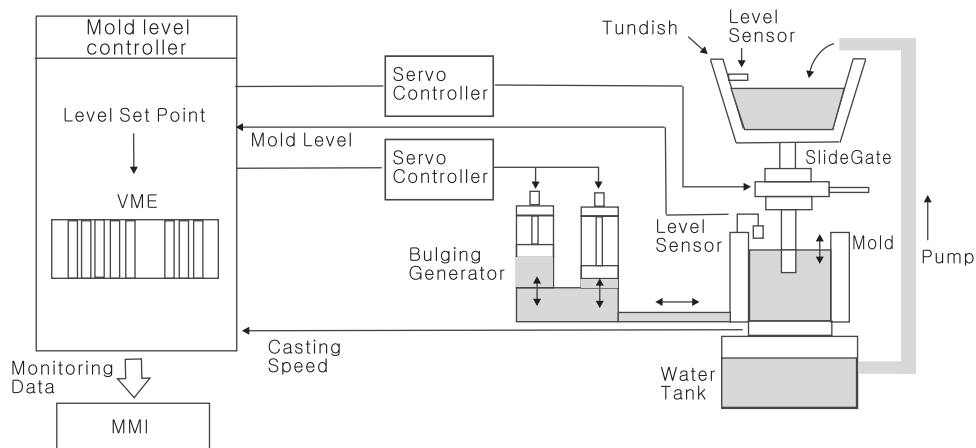


Fig. 10. Configuration of the proposed control system.

bulging used for simulation consisted of two sinusoids with amplitude 10.5 mm peak to peak and frequencies 0.120–0.122 and 0.140–0.142 Hz. The phase of the bulging disturbance was assumed to be 0° . The learning gain $L(k)$ was set to 0.6 for all $k \in \mathbb{N}$, the forgetting factor to $p=0.2$ and eight periods were simulated under bulging disturbance.

In this simulation, the level error increased to 13 mm peak to peak when the PID controller is used but it went down to ~ 7 mm peak to peak when the P-type ILC is applied. However, after 4th iterations, the control performance was not improved further due to time varying characteristics of the bulging disturbance (Fig. 7). When the proposed ILC was used, the controller performance was continuously improved even after 4th iterations (Fig. 8).

Fig. 9 shows the behavior of switching parameter $s_2(k)$ and the proposed controller output. When $s_2(k)=0$, the switch is turned on, but otherwise, it is turned off. As shown in Figs. 8 and 9, the switch turns on when the absolute value of the present error exceeds the threshold value T_v (4 mm) and prevents the proposed controller from responding to the unexpected peak. In addition, the proposed controller output generates bulging signal estimates and used them to reduce the original bulging disturbance.

5. Experimental results

A 1/4 scale H/W simulator is built to test the molten steel level algorithm experimentally using a model system (Figs. 10 and 11) and



Fig. 11. 1/4 scale H/W simulator.

executed the control program on a VME system with a VxWorks O/S. The control software was programmed with a Programmable Logic Controller (PLC) in which Ladder Diagram (LD), Function Block Diagram (FBD) and C programming are available. The H/W simulator uses water instead of molten steel and includes an artificial bulging generator to produce the bulging disturbance. Tundish, mold, bulging generator and water tank are the main parts of the H/W simulator. To produce the bulging disturbance, the two servo motors were used. When these motors move up and down, water exits and enters the mold through a pipe. The two motors were oscillated regularly, each at a different frequency, to produce bulging in the shape of two sine waves. The water level in the mold was measured using an ultrasonic sensor.

The input side of the H/W simulator consists of a slide gate, and two motors to induce bulging. The output side of the simulator consists of the mold level, the slide gate position, and the limit sensors. A servo motor was used to control the position of the slide gate. A manual valve was placed beneath the mold to control the outgoing flow from the mold into the water tank and its flow speed was output as an electrical signal.

To compare the control performance of the H/W simulator, it is tested using a PID controller, a PID controller with a P-type iterative learning algorithm, and a PID controller with the proposed iterative learning algorithm. For all three cases, the reference mold level was

set to 80 mm; the bulging signal consisted of sine waves with amplitude 11.7 mm peak to peak and frequencies 0.124–0.128 and 0.140–0.144 Hz.

To compare the performances of the PID controller and the PID controller with a P-type iterative learning algorithm, the learning gain $L(k)$ was set to 0.4 for all $k \in \mathbb{N}$ and eight iterations were performed. Under the bulging disturbance, the PID controller with P-type iterative learning algorithm performed better than the PID controller (Fig. 12). With only the PID controller, the level error increased to 13 mm peak to peak but with the P-type iterative learning controller this error was only ~ 8 mm peak to peak. However, after five iterations, the control performance gradually declined mainly due to time-varying characteristics of the bulging disturbance.

To compare the performances of the PID controller, and the PID controller with the proposed iterative learning algorithm, the learning gain $L(k)$ was set to 0.4 for all $k \in \mathbb{N}$, the forgetting factor to $p=0.2$ and eight iterations were performed. The controller with the proposed iterative learning controller performed better than the other two controllers (Fig. 13, Table 1). Even after five iterations, control quality was maintained despite the time-varying characteristics of the bulging disturbance. The P-type iterative learning controller reduced the peak to peak level error to ~ 8 mm, but the proposed controller reduced it to ~ 5 mm. The quality of the slab in the continuous

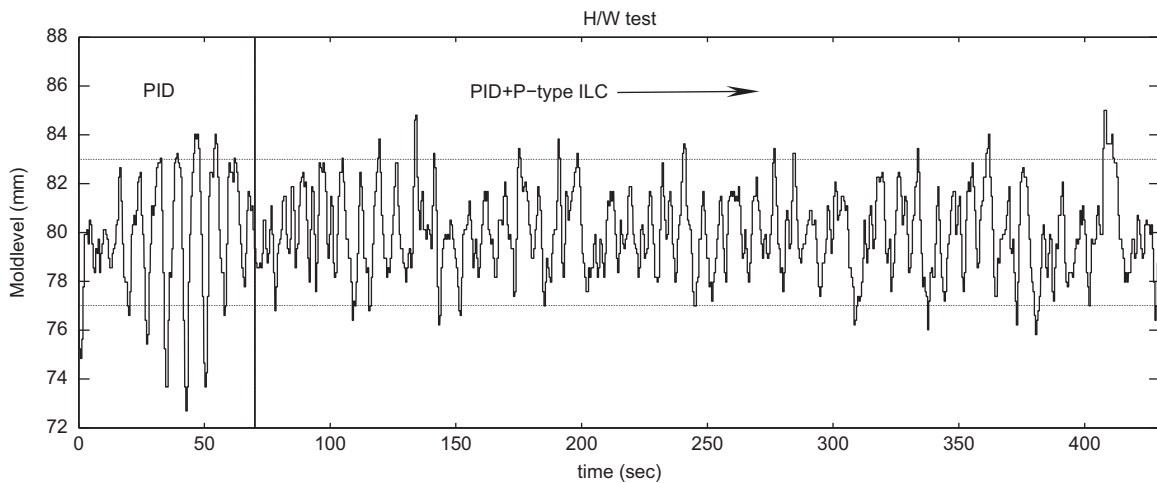


Fig. 12. Mold level when PID and PID + P-type ILC controllers are used.

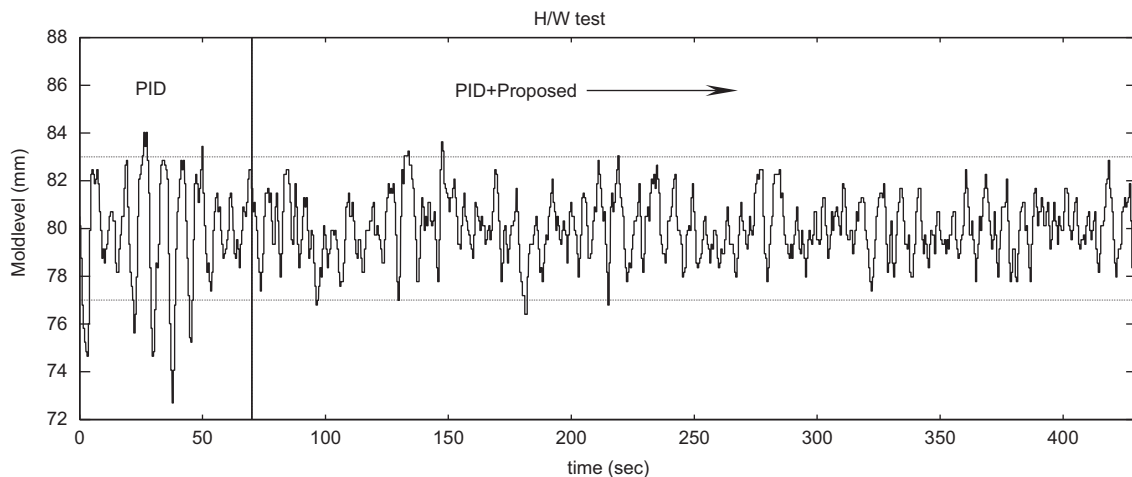


Fig. 13. Mold level when PID and PID + Proposed controller are used.

Table 1
Precision of controllers tested, means of eight iterations.

Controller	Level performance (%) within specified limits		
	$\leq \pm 3$ mm	$\leq \pm 5$ mm	$\leq \pm 10$ mm
PID	79.73	94.90	100
PID + P-type ILC	93.31	100	100
PID + Proposed	98.10	100	100

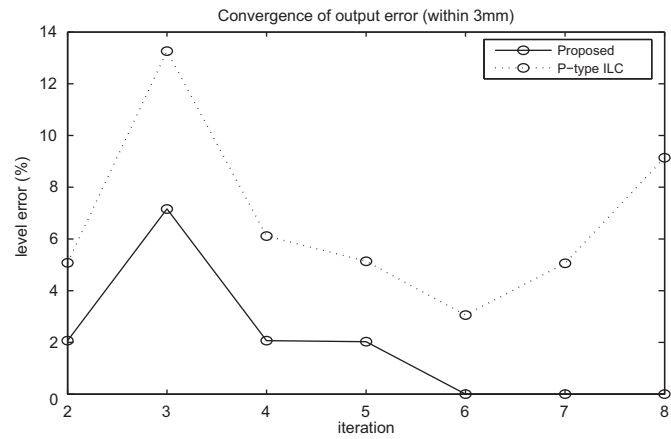


Fig. 14. The percentage of mold level error whose magnitude is ≥ 3 mm.

casting process is usually considered good when the molten steel level stays within 3 mm of the reference level. The proposed controller achieved this precision $> 98\%$ of the time (Table 1).

Using this controller, the mold level error eventually converged to $\leq \pm 3$ mm (Fig. 14). Within six iterations, the mold level error of the control system with the proposed ILC or with the P-type learning controller tended to decrease. The mold level performance with the P-type learning controller tended to become less precise after seven iterations, as a result of time-varying disturbances and model uncertainties. But the mold level with the proposed ILC learning controller remained acceptably precise even in the presence of these time-varying disturbances and model uncertainties.

6. Conclusion

In this paper, an iterative learning control technique was proposed and applied to a continuous casting simulator. Treating one period of bulging disturbance as one iteration, it is developed an iterative learning controller that performs well in reducing the periodic bulging disturbance. In the presence of model uncertainties, disturbances, noises and initial errors, it is proved that the state signal error, the output signal error and the input signal error of the control system are ultimately bounded. The proposed control method was implemented on a 1/4 scale H/W simulator but it will soon be applied to a full scale H/W simulator in an active steel mill.

Acknowledgements

This research was supported by Ministry of Knowledge and Economy, Republic of Korea, under the ITRC (Information Technology Research Center) support program supervised by IITA (Institute for Information Technology Advancement) (IITA-2009-C1090-0901-0004), and this research was also supported by POSCO (Pohang Iron and Steel Co.).

Appendix A. Stability analysis of the controller

In this Appendix, the stability and boundedness of the proposed ILC scheme is considered as applied to the process of regulating molten steel level. When the system suffers from model uncertainties, periodic bulging disturbances, output noises and initial state errors, it can be proved that $\|x_d(k) - x_i(k)\|$, $\|u_d(k) - u_i(k)\|$ and $\|y_d(k) - y_i(k)\|$ are ultimately bounded as given in the following theorem. For subsequent analysis, b_s , b_{s_1} and b_{s_2} are defined as follows:

Definition 1.

$$b_s = \max_{1 \leq i < \infty} \max_{1 \leq k \leq n} \|(1 - s_{i1}(k)(1 - p))\|,$$

$$b_{s_1} = \max_{1 \leq i < \infty} \max_{1 \leq k \leq n} \|s_{i1}(k)\|,$$

$$b_{s_2} = \max_{1 \leq i < \infty} \max_{1 \leq k \leq n} \|s_{i2}(k)\|.$$

Theorem 1. Consider a time-varying discrete-time system (5) with an iterative learning rule (8). Assume that Assumptions 1–3 are satisfied and that the inequality

$$\|s_{i1}(k)(1 - p)\| + b_{s_1} b_L c_B \leq \rho < 1, \quad (9)$$

holds for all $(x_i(k), k) \in \mathbb{R}^n \times \mathbb{N}$. Given a bounded output sequence $y_d(k)$ in the presence of model uncertainties, bulging disturbances, output noises and initial state errors, $\|u_i(k) - u_d(k)\|$, $\|x_i(k) - x_d(k)\|$, and $\|y_i(k) - y_d(k)\|$ will be ultimately bounded with bounds that are functions of b_β , b_d , b_n , b_{x_0} .

Remark 1. Note that p and b_L are the design parameters and these parameters can be selected to satisfy (9).

Proof. Subtracting $x_d(k+1)$ from $x_i(k+1)$ yields

$$\begin{aligned} \tilde{x}_i(k+1) &= x_d(k+1) - x_i(k+1) \\ &= [x_d(k) + B(x_d(k), u_d(k), k)] - [x_i(k) + B(x_i(k), u_i(k), k) + \beta_i(k) + d_i(k)] \\ &= \tilde{x}_i(k) + B(x_d(k), u_d(k), k) - B(x_i(k), u_i(k), k) - \beta_i(k) - d_i(k), \end{aligned} \quad (10)$$

where $\tilde{x}_i(k) = x_d(k) - x_i(k)$ is the state error vector.

Taking norms on both sides of (10) gives

$$\|\tilde{x}_i(k+1)\| \leq \|\tilde{x}_i(k)\| + c_B \|\tilde{x}_i(k)\| + c_B \|\tilde{u}_i(k)\| + b_\beta + b_d, \quad (11)$$

where $\tilde{u}_i(k) = u_d(k) - u_i(k)$.

Then it follows from (11) that

$$\|\tilde{x}_i(k+1)\| \leq (1 + c_B) \|\tilde{x}_i(k)\| + c_B \|\tilde{u}_i(k)\| + b_\beta + b_d, \quad (12)$$

which yields

$$\|\tilde{x}_i(k)\| \leq \sum_{j=0}^{k-1} (1 + c_B)^{k-1-j} [c_B \|\tilde{u}_i(j)\| + b_\beta + b_d] + (1 + c_B)^k b_{x_0}. \quad (13)$$

On the other hand, (8) indicates that the control input error vector $\tilde{u}_{i+1}(k)$ becomes

$$\begin{aligned} \tilde{u}_{i+1}(k) &= u_d(k) - u_{i+1}(k) \\ &= u_d(k) - s_{i1}(k)[(1 - p)u_i(k) + L(k)e_i(k+1)] - s_{i2}(k)u_{i+1}(k-1) \\ &= u_d(k) - s_{i1}(k)(1 - p)u_i(k) - s_{i1}(k)(1 - p)u_d(k) \\ &\quad + s_{i1}(k)(1 - p)u_d(k) - s_{i1}(k)L(k)e_i(k+1) - s_{i2}(k)u_{i+1}(k-1) \\ &= s_{i1}(k)(1 - p)\tilde{u}_i(k) + u_d(k) - s_{i1}(k)(1 - p)u_d(k) \\ &\quad - s_{i1}(k)L(k)[y_d(k+1) - y_i(k+1)] - s_{i2}(k)u_{i+1}(k-1) \\ &= s_{i1}(k)(1 - p)\tilde{u}_i(k) + (1 - s_{i1}(k)(1 - p))u_d(k) \\ &\quad - s_{i1}(k)L(k)[x_d(k+1) - x_i(k+1) - n_i(k)] - s_{i2}(k)u_{i+1}(k-1) \\ &= s_{i1}(k)(1 - p)\tilde{u}_i(k) + (1 - s_{i1}(k)(1 - p))u_d(k) - s_{i1}(k)L(k)[x_d(k) \\ &\quad + B(x_d(k), u_d(k), k) - x_i(k) - B(x_i(k), u_i(k), k) - \beta_i(k) - d_i(k) \\ &\quad - n_i(k)] - s_{i2}(k)u_{i+1}(k-1) + s_{i2}(k)u_d(k-1) - s_{i2}(k)u_d(k-1) \\ &= s_{i1}(k)(1 - p)\tilde{u}_i(k) + (1 - s_{i1}(k)(1 - p))u_d(k) - s_{i1}(k)L(k)[\tilde{x}_i(k) \\ &\quad + B(x_d(k), u_d(k), k) - B(x_i(k), u_i(k), k) - \beta_i(k) - d_i(k) - n_i(k)] \\ &\quad + s_{i2}(k)\tilde{u}_{i+1}(k-1) - s_{i2}(k)u_d(k-1) \end{aligned}$$

$$\begin{aligned}
 &= s_{i1}(k)(1-p)\tilde{u}_i(k) + (1-s_{i1}(k)(1-p))u_d(k) \\
 &\quad - s_{i1}(k)L(k)\tilde{x}_i(k) - s_{i1}(k)L(k)[B(x_d(k), u_d(k), k) - B(x_i(k), u_i(k), k)] \\
 &\quad + s_{i1}(k)L(k)[\beta_i(k) + d_i(k) + n_i(k)] + s_{i2}(k)\tilde{u}_{i+1}(k-1) - s_{i2}(k)u_d(k-1)
 \end{aligned} \tag{14}$$

Applying Property 2 and Assumption 2 to (14) yields

$$\begin{aligned}
 \|\tilde{u}_{i+1}(k)\| \leq & \|s_{i1}(k)(1-p)\| \|\tilde{u}_i(k)\| + b_s b_{u_d} + b_{s_1} b_L \|\tilde{x}_i(k)\| + b_{s_1} b_L c_B \|\tilde{x}_i(k)\| \\
 & + b_{s_1} b_L c_B \|\tilde{u}_i(k)\| + b_{s_1} b_L (b_\beta + b_d + b_n) + b_{s_2} \|\tilde{u}_{i+1}(k-1)\| + b_{s_2} b_{u_d}.
 \end{aligned} \tag{15}$$

Let $h_1 = b_{s_1} b_L (1 + c_B)$ and $b_1 = (b_s + b_{s_2}) b_{u_d} + b_{s_1} b_L (b_\beta + b_d + b_n)$. Then (15) can be rewritten as

$$\begin{aligned}
 \|\tilde{u}_{i+1}(k)\| \leq & [\|s_{i1}(k)(1-p)\| + b_{s_1} b_L c_B] \|\tilde{u}_i(k)\| + h_1 \|\tilde{x}_i(k)\| \\
 & + b_{s_2} \|\tilde{u}_{i+1}(k-1)\| + b_1.
 \end{aligned} \tag{16}$$

Substituting (11) and (9) into (16) gives

$$\begin{aligned}
 \|\tilde{u}_{i+1}(k)\| \leq & \rho \|\tilde{u}_i(k)\| + h_1 \left[\sum_{j=0}^{k-1} (1+c_B)^{k-1-j} [c_B \|\tilde{u}_i(j)\| + b_\beta + b_d] + (1+c_B)^k b_{x_0} \right] \\
 & + b_{s_2} \|\tilde{u}_{i+1}(k-1)\| + b_1.
 \end{aligned} \tag{17}$$

Multiplying both sides of (17) by $(1/\alpha)^k$ to compute the α -norm yields

$$\begin{aligned}
 \|\tilde{u}_{i+1}(k)\| \left(\frac{1}{\alpha}\right)^k \leq & \rho \|\tilde{u}_i(k)\| \left(\frac{1}{\alpha}\right)^k + h_1 b_{x_0} \left(\frac{1+c_B}{\alpha}\right)^k + b_1 \left(\frac{1}{\alpha}\right)^k \\
 & + \left(\frac{h_1}{\alpha}\right) \sum_{j=0}^{k-1} \left(\frac{1+c_B}{\alpha}\right)^{k-1-j} \left[c_B \|\tilde{u}_i(j)\| \left(\frac{1}{\alpha}\right)^j + (b_\beta + b_d) \left(\frac{1}{\alpha}\right)^j \right] \\
 & + b_{s_2} \left(\frac{1}{\alpha}\right) \|\tilde{u}_{i+1}(k-1)\| \left(\frac{1}{\alpha}\right)^{k-1}.
 \end{aligned} \tag{18}$$

Taking $\alpha > \max[1, b_\beta + b_d]$ yields

$$\begin{aligned}
 \|\tilde{u}_{i+1}\|_\alpha \leq & \rho \|\tilde{u}_i\|_\alpha + h_1 b_{x_0} \left(\frac{1+c_B}{\alpha}\right)^k + b_1 \left(\frac{1}{\alpha}\right)^k \\
 & + (b_B \|\tilde{u}_i\|_\alpha + b_\beta + b_d) \left(\frac{h_1}{\alpha}\right) \sum_{j=0}^{k-1} \left(\frac{1+c_B}{\alpha}\right)^{k-1-j} + \left(\frac{b_{s_2}}{\alpha}\right) \|\tilde{u}_{i+1}\|_\alpha \\
 \leq & \rho \|\tilde{u}_i\|_\alpha + h_1 b_{x_0} \left(\frac{1+c_B}{\alpha}\right)^k + b_1 \left(\frac{1}{\alpha}\right)^k \\
 & + (b_B \|\tilde{u}_i\|_\alpha + b_\beta + b_d) \left(\frac{h_1 [1 - ((1+c_B)/\alpha)^k]}{\alpha - (1+c_B)}\right) + \left(\frac{b_{s_2}}{\alpha}\right) \|\tilde{u}_{i+1}\|_\alpha \\
 = & \left(\frac{\alpha}{\alpha - b_{s_2}}\right) \left(\rho + b_B h_1 \frac{1 - ((1+c_B)/\alpha)^k}{\alpha - (1+c_B)}\right) \|\tilde{u}_i\|_\alpha \\
 & + \left(\frac{\alpha h_1}{\alpha - b_{s_2}}\right) \left(\frac{1+c_B}{\alpha}\right)^k b_{x_0} + \frac{\alpha b_1}{\alpha - b_{s_2}} \left(\frac{1}{\alpha}\right)^k \\
 & + \frac{\alpha (b_\beta + b_d) h_1 [1 - ((1+c_B)/\alpha)^k]}{(\alpha - b_{s_2})(\alpha - (1+c_B))}
 \end{aligned} \tag{19}$$

because

$$\frac{1}{\alpha} \sum_{j=0}^{k-1} \left(\frac{1+c_B}{\alpha}\right)^{k-1-j} = \frac{((1+c_B)/\alpha)^{k-1} ((\alpha/(1+c_B))^k - 1)}{\alpha(\alpha/(1+c_B) - 1)} = \frac{1 - ((1+c_B)/\alpha)^k}{\alpha - (1+c_B)}. \tag{20}$$

Then (19) implies

$$\|\tilde{u}_{i+1}\|_\alpha \leq \hat{\rho} \|\tilde{u}_i\|_\alpha + \varepsilon, \tag{21}$$

where

$$\hat{\rho} = \left(\frac{\alpha}{\alpha - b_{s_2}}\right) \left(\rho + b_B h_1 \frac{1 - ((1+c_B)/\alpha)^k}{\alpha - (1+c_B)}\right), \tag{22}$$

$$\varepsilon = \left(\frac{\alpha h_1}{\alpha - b_{s_2}}\right) \left(\frac{1+c_B}{\alpha}\right)^k b_{x_0} + \frac{\alpha b_1}{\alpha - b_{s_2}} \left(\frac{1}{\alpha}\right)^k + \frac{\alpha (b_\beta + b_d) h_1 [1 - ((1+c_B)/\alpha)^k]}{(\alpha - b_{s_2})(\alpha - (1+c_B))}, \tag{23}$$

and then

$$\|\tilde{u}_{i+1}\|_\alpha \leq \hat{\rho}^i \|\tilde{u}_1\|_\alpha + \varepsilon \sum_{j=0}^{i-1} \hat{\rho}^j = \hat{\rho}^i \|\tilde{u}_1\|_\alpha + \varepsilon (1 - \frac{\hat{\rho}^i}{1 - \hat{\rho}}).$$

If α is chosen to be large enough that $\hat{\rho} < 1$,

$$\lim_{i \rightarrow \infty} \|\tilde{u}_i\|_\alpha \leq \frac{\varepsilon}{1 - \hat{\rho}}. \tag{24}$$

Similarly, multiplying both sides of (13) by $(1/\alpha)^k$ gives

$$\begin{aligned}
 \|\tilde{x}_i(k)\| \left(\frac{1}{\alpha}\right)^k \leq & \left(\frac{1}{\alpha}\right) \sum_{j=0}^{k-1} \left(\frac{1+c_B}{\alpha}\right)^{k-1-j} \left[c_B \|\tilde{u}_i(j)\| \left(\frac{1}{\alpha}\right)^j + (b_\beta + b_d) \left(\frac{1}{\alpha}\right)^j \right] \\
 & + \left(\frac{1+c_B}{\alpha}\right)^k b_{x_0},
 \end{aligned} \tag{25}$$

gives

$$\begin{aligned}
 \|\tilde{x}_i\|_\alpha \leq & (c_B \|\tilde{u}_i\|_\alpha + b_\beta + b_d) \frac{1 - ((1+c_B)/\alpha)^k}{\alpha - (1+c_B)} + \left(\frac{1+c_B}{\alpha}\right)^k b_{x_0} \\
 = & c_B \frac{1 - ((1+c_B)/\alpha)^k}{\alpha - (1+c_B)} \|\tilde{u}_i\|_\alpha + (b_\beta + b_d) \frac{1 - ((1+c_B)/\alpha)^k}{\alpha - (1+c_B)} \\
 & + \left(\frac{1+c_B}{\alpha}\right)^k b_{x_0}.
 \end{aligned} \tag{26}$$

Applying (24) into (26),

$$\begin{aligned}
 \lim_{i \rightarrow \infty} \|\tilde{x}_i\|_\alpha \leq & c_B \frac{1 - ((1+c_B)/\alpha)^k}{\alpha - (1+c_B)} \frac{\varepsilon}{1 - \hat{\rho}} \\
 & + (b_\beta + b_d) \frac{1 - ((1+c_B)/\alpha)^k}{\alpha - (1+c_B)} + \left(\frac{1+c_B}{\alpha}\right)^k b_{x_0}.
 \end{aligned} \tag{27}$$

Next, subtracting (5) from (6) gives

$$\tilde{y}_i(k) = y_d(k) - y_i(k) = x_d(k) - [x_i(k) + n_i(k)] = \tilde{x}_i(k) - n_i(k). \tag{28}$$

Taking norms and multiplying both sides of (28) by $(1/\alpha)^k$ yields

$$\|\tilde{y}_i\|_\alpha \leq \|\tilde{x}_i\|_\alpha + \left(\frac{1}{\alpha}\right)^k b_n. \tag{29}$$

Substituting (27) into (29) gives

$$\begin{aligned}
 \lim_{i \rightarrow \infty} \|\tilde{y}_i\|_\alpha \leq & c_B \frac{1 - ((1+c_B)/\alpha)^k}{\alpha - (1+c_B)} \frac{\varepsilon}{1 - \hat{\rho}} + (b_\beta + b_d) \frac{1 - ((1+c_B)/\alpha)^k}{\alpha - (1+c_B)} \\
 & + \left(\frac{1+c_B}{\alpha}\right)^k b_{x_0} + \left(\frac{1}{\alpha}\right)^k b_n.
 \end{aligned} \tag{30}$$

Consequently, in the presence of model uncertainties, bulging disturbances, output noises and initial state errors, the errors $\|u_i(k) - u_d(k)\|$, $\|x_i(k) - x_d(k)\|$ and $\|y_i(k) - y_d(k)\|$ become ultimately bounded by functions of b_β , b_d , b_n , b_{x_0} as given in (24), (27), and (30). \square

Appendix B. Supplementary material

Supplementary data associated with this article can be found in the online version of 10.1016/j.conengprac.2010.11.009.

References

- Barron, M. A., Aguilar, R., Gonzalez, J., & Melendez, E. (1998). Model-based control of mold level in a continuous steel caster under model uncertainties. *Control Engineering Practice*, 6(2), 191–196.
- Chien, C.-J., & Liu, J.-S. (1994). A P-type iterative learning controller for robust output tracking of nonlinear time-varying systems. In *American control conference June, USA* (pp. 2595–2599).
- Doh, T.-Y., Ryoo, J. R., & Chung, M. J. (2006). Design of a repetitive controller: an application to the track-following servo system of optical disk drives. *IEE Proceedings Control Theory and Applications*, 153(3), 323–330.
- Dussud, M., Galichet, S., & Foulloy, L. P. (1998). Application of fuzzy logic control for continuous casting mold level control. *IEEE Transactions on Control Systems Technology*, 6(2), 246–256.
- Furtmueller, C., & Gruenbacher, E. (2006). Suppression of periodic disturbances in continuous casting using an internal model predictor. In *Proceedings of the 2006 IEEE international conference on control applications*, Munich, Germany.
- Hauser, J. (1987). Learning control for a class of nonlinear systems. In *26th IEEE conference on decision and control* (pp. 859–860).
- Heinzinger, G., Fenwick, D., Paden, B., & Miyazaki, F. (1992). Stability of learning control with disturbances and uncertain initial conditions. *IEEE Transactions on Automatic Control*, 37(1), 110–114.
- Jang, T.-J., Choi, C.-H., & Ahn, H.-S. (1995). Iterative learning control in feedback systems. *Automatica*, 31(2), 243–248.
- Kang, M. K., Lee, J. S., & Han, K. L. (2005). Kinematic path-tracking of mobile robot using iterative learning control. *Journal of Robotic Systems*, 22(2), 111–121.
- Keyser, R. (1991). Improved mould-level control in a continuous steel casting line. *Control Engineering Practice*, 5(2), 231–237.
- Kuc, T.-Y., Lee, J. S., & Nam, K. (1992). An iterative learning control theory for a class of nonlinear dynamic systems. *Automatica*, 28(6), 1215–1221.
- Lee, D., Kueon, Y., & Lee, S. (2003). High performance hybrid mold level controller for thin slab caster. *Control Engineering Practice*, 12(3), 275–281.
- Moon, J.-H., Lee, M.-N., & Chung, M. J. (1998). Repetitive control for the track-following servo system of an optical disk drive. *IEEE Transactions on Control Systems Technology*, 6(5), 663–670.
- Wang, D. (1998). Convergence and robustness of discrete time nonlinear systems with iterative learning control. *Automatica*, 34(11), 1445–1448.
- Watanabe, T., Omura, K., Konishi, M., Watanabe, S., & Furukawa, K. (1999). Mold level control in continuous caster by neural network model. *ISIJ International*, 39(10), 1053–1060.